

^{113}Cd Nuclear Magnetic Resonance Spectroscopy of Cd^{2+} -Substituted Heme and Myoglobin

Michael A. Kennedy and Paul D. Ellis*

Contribution from the Department of Chemistry, University of South Carolina, Columbia, South Carolina 29208. Received August 25, 1988

Abstract: Solution- and solid-state ^{113}Cd NMR spectra have been obtained at 7.1 and 9.4 T for precursors of Cd^{2+} -substituted hemoglobin, namely, cadmium protoporphyrin IX dimethyl ester (Cd-PPIXDME), cadmium protoporphyrin IX (Cd-PPIX), i.e., Cd^{2+} -substituted heme, and Cd^{2+} -substituted myoglobin (Cd-Mb). The isotropic chemical shift in solution for these complexes ranged from 375 ppm in Cd-PPIX to 455 ppm in Cd-Mb. The resonance for each of the above was observed to be temperature dependent in solution and is analyzed in terms of chemical-exchange equilibria. Rate and equilibrium constants are calculated for select cases. Chemical shielding tensor parameters were obtained via solid-state ^{113}Cd NMR experiments (with and without magic-angle spinning) for each of the complexes above in addition to the pyridyl adduct of Cd-PPIXDME (Cd-PPIXDME-PYR). The greatest deviation from axial symmetry occurred in Cd-PPIXDME-PYR with asymmetry, $\eta = 0.32$. The chemical shift anisotropy, however, ranged from $\Delta\sigma = +423$ ppm in Cd-PPIXDME to ~ -200 ppm for Cd-Mb. The isotropic chemical shift ranged in solid state from 365 ppm for Cd-PPIX to 480 ppm for Cd-PPIXDME and Cd-PPIXDME-PYR.

To date, ^{113}Cd NMR has been utilized in both solution and solid state to examine the metal environment in calcium, cadmium, manganese, magnesium, and zinc-containing proteins, e.g., parvalbumin, concanavalin A, skeletal troponin C, superoxide dismutase, metallothionein, etc. Summers¹ has recently reviewed the progress in ^{113}Cd NMR in comprehensive detail. The ^{113}Cd chemical shift range of over 900 ppm affords a probe that is extremely sensitive to the metal coordination geometry and ligand type. However, investigation of cadmium-substituted hemoproteins has not been documented. Iron-protoporphyrin IX (heme) constitutes the prosthetic group of the respiratory proteins myoglobin and hemoglobin.² Iron-containing porphyrin derivatives (hemes), e.g., heme A, are prosthetic groups for the family of cytochromes involved in oxidative phosphorylation.³ Photosynthetic systems depend on magnesium-containing porphyrins for conversion of light energy to chemical energy.^{4,5} In each of these protein families, the function of the protein is centered at the metal site in the porphyrin.

Previously, Jakobsen et al.⁶ investigated cadmium mesotetraphenylporphyrin (Cd-TTP) and its pyridyl adduct (PY-Cd-TTP) as model compounds for cadmium-substituted myoglobin and hemoglobin. One of the striking results was that a deceptively small 33 ppm isotropic chemical shift between Cd-TTP and PY-Cd-TTP originated from large compensating changes, i.e., ~ 230 ppm, of the individual shielding tensor elements. The increased electronic perturbation of the Cd^{2+} ion due to the axial pyridine ligation accounted for 112 ppm deshielding of σ_{\perp} and the decreased in-plane perturbation associated with the pulling of the cadmium atom out of the plane accounted for the 124 ppm shielding of σ_{\parallel} . The sensitivity of the ^{113}Cd shielding tensor elements to the axial ligation state of cadmium porphyrins makes cadmium-substituted hemoproteins potentially very informative systems with which to investigate dynamics and electronic interactions at "active sites" of these oxygen transport and electron transfer proteins. Structural changes accompanying the cooperative binding of oxygen,^{7,8} competitive binding of poisons,^{7,8} or

stabilizing binding of cross-linking agents^{7,8} in cadmium hybrid hemoglobins should be sensitively monitored by ^{113}Cd chemical shift tensors observed by solid-state NMR. With the intention of expanding the utility of ^{113}Cd NMR into the realm of hemoproteins, we have investigated cadmium protoporphyrin IX dimethyl ester (Cd-PPIXDME), cadmium protoporphyrin IX (Cd-PPIX), and cadmium myoglobin (Cd-Mb) as precursors of cadmium-substituted hemoglobins. The structures of Cd-PPIXDME and Cd-PPIX are represented in Figure 1.

Experimental Section

Synthesis. Cd-PPIXDME. Protoporphyrin IX dimethyl ester (Sigma), used without further purification, was dissolved in dimethylformamide (~ 40 mL/0.25 g of porphyrin). A 20% mole excess of cadmium acetate dihydrate (Aldrich) was dissolved in an equal volume of dimethylformamide. The two solutions were mixed and heated at ~ 80 °C until metalation was complete as monitored by the disappearance of the visible absorption bands at 505 and 630 nm present in the unmetallated porphyrin (see Figure 2). The reaction typically is complete within 45 min. The reaction mixture was then cooled to 4.5 °C by refrigeration. A threefold volume of deionized water was added to the reaction mixture in a separatory funnel, and the metallated porphyrin was isolated by extraction with diethyl ether until the ether layer remained colorless. The ether fractions were pooled and successively extracted with deionized water until addition of Na_2S solution to the aqueous fraction remained colorless. A yellow color indicated the presence of residual cadmium. The ether fraction was dried over an excess of NaOH and then decanted through filter paper. Cd-PPIXDME was crystallized overnight by slow evaporation of the ether solution.

Cd-PPIXDME-PYR. Crystals of Cd-PPIXDME-PYR were obtained by evaporation of an ether solution of Cd-PPIXDME in the presence of a 100 M excess of pyridine.

Cd-PPIX. Cd-PPIXDME, prepared as above, was dissolved in pyridine (~ 40 mL/0.25 g of porphyrin). A 20% mole excess of KOH was added in $\sim 1/3$ volume of aqueous solution. The hydrolysis reaction, carried out at room temperature, was monitored by reverse-phase TLC using Baker plates. A developing solution of a 70/30 mixture of methanol/water was used. Unhydrolyzed porphyrin did not move from the application spot, i.e., $R_f = 0.0$, whereas hydrolyzed porphyrin had an $R_f = 0.45$. An intermediate hydrolysis product, Cd-protoporphyrin IX monomethyl ester, was also present at $R_f = 0.2$ when hydrolysis was

(1) M. Summers *Coord. Chem. Rev.* **1988**, *86*, 43-134.

(2) Antonini, E.; Brunori, M. *Hemoglobin and Myoglobin in Their Reactions with Ligands*; Elsevier: New York, 1971.

(3) Lemberg, R.; Barrett, J. *Cytochrome*; Academic Press: New York, 1973.

(4) Vernon, L. D.; Seely, G. R., Eds. *The Chlorophylls*; Academic Press: New York, 1966.

(5) Clayton, R. K.; Sistrom, W. R., Eds. *The Photosynthetic Bacteria*; Plenum Press: New York, 1978.

(6) Jakobsen, H. J.; Ellis, P. D.; Inners, R. R.; Jensen, C. F. *J. Am. Chem. Soc.* **1982**, *104*, 7442.

(7) (a) Perutz, M. A. *Nature* **1970**, *228*, 726. (b) Hopfield, J. J. *J. Mol. Biol.* **1973**, *77*, 207. (c) Gelin, B. R.; Karplus, M. *Proc. Natl. Acad. Sci. U.S.A.* **1977**, *74*, 801. (d) Baldwin, J.; Chothia, C. *J. Mol. Biol.* **1979**, *129*, 175. (e) Kilmartin, J. V.; Rossi-Bernardi, L. *Physiol. Rev.* **1973**, *53*, 836. (f) Kilmartin, J. V. *Br. Med. Bull.* **1976**, *32*, 209. (g) Benesch, R.; Benesch, R. E. *Nature* **1969**, *221*, 618. (h) Lenfant, C.; Torrence, J. D.; Woodson, R. D.; Jacobs, P.; Finch, C. A. *Fed. Proc., Fed. Am. Soc. Exp. Biol.* **1970**, *29*, 1115. (i) Tyuma, I.; Shimizu, K. *Fed. Proc., Fed. Am. Soc. Exp. Biol.* **1970**, *29*, 1112.

(8) Perutz, M. F. *Sci. Am.* **1978**, *239*, 92.

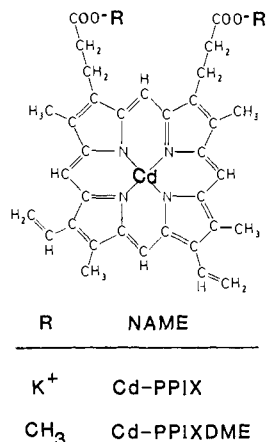


Figure 1. Structural formulas for cadmium protoporphyrin IX (Cd-PPIX) and cadmium protoporphyrin IX dimethyl ester (Cd-PPIXDME).

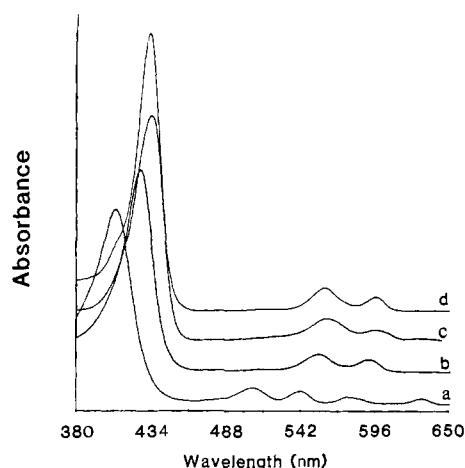


Figure 2. Visible spectrum at 16 °C of (a) a 4.0 μ M solution of PPIXDME in CHCl_3 , (b) a 3.4 μ M solution of Cd-PPIXDME in CHCl_3 , (c) a 3.4 μ M solution of Cd-PPIXDME in DMF, and (d) a 3.4 μ M solution of Cd-PPIXDME in pyridine (see Table I).

incomplete. By successive spottings, the hydrolysis reaction was observed to be complete when a single component at $R_f = 0.45$ is observed under a UV lamp. The Cd-PPIX was precipitated with an excess of pyridine, isolated by centrifugation, and dried under vacuum in an Abderhalden pistol at 160 °C.

Cd-Mb. Apomyoglobin was prepared by the method of Yonetani.⁹ A stoichiometric titration, shown in Figure 3, was done to demonstrate stoichiometric binding of Cd-PPIX to apomyoglobin. A stoichiometric amount of [¹¹³Cd]PPIX, prepared with 95.3% isotopically pure ¹¹³Cd (U.S. Services, Inc.) in acetate form, was added to apomyoglobin in 0.2 M $\text{Na}_2\text{B}_4\text{O}_7$ buffer at pH 9.4. Unbound [¹¹³Cd]PPIX was removed by extensive dialysis with borate buffer. Concentration of ~ 0.2 g of Cd-Mb to 2.5 mL for NMR solution samples was achieved by a Amicon ultrafiltration unit. Approximately 1/4 volume of D_2O was added as a lock solvent and the sample reconcentrated for observation. Solid-state samples were prepared by dialysis of Cd-Mb with pH 9.4 H_2O and then lyophilized. The lyophilized protein was then used directly or reequilibrated with D_2O to an extent of 0.2 g of D_2O /g of protein following the procedure of Marchetti et al.¹⁰

Characterization. Reversed-phase thin-layer chromatography (RPTLC). The purity of each porphyrin complex was confirmed by RPTLC on Baker Si-C₁₈F TLC plates. After isolation of Cd-PPIXDME as described above, a single component, $R_f = 0.28$, was observed by using a 95/5 developing solution of acetonitrile/chloroform. Cd-PPIX was developed with a 70/30 solution of air-saturated methanol/water. A single component was observed at $R_f = 0.45$.

UV-Visible Spectrophotometry. UV-visible spectra were obtained on a Varian DMS 200 UV-visible spectrophotometer. Figure 2b-d shows the UV-visible spectrum of Cd-PPIXDME in chloroform, pyridine, and

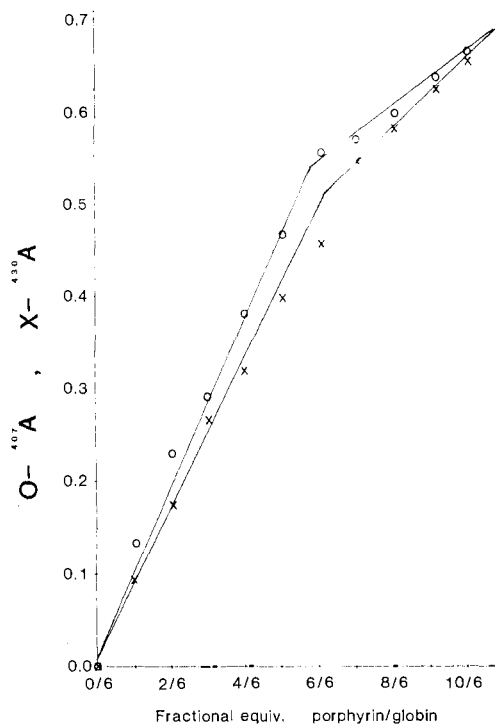


Figure 3. Stoichiometric titration plot of apomyoglobin with O-hemin in 0.1 M phosphate buffer at pH = 6.8 monitored by change in absorption at 407 nm and X-Cd-PPIX in 0.1 M borate buffer at pH = 9.4 monitored by change in absorption at 430 nm.

Table I. Summary of UV-Visible Spectrophotometric Data for Cd-PPIXDME, Cd-PPIX, and Cd-Mb

compd	solvent	pH	λ_{max} , nm	$\epsilon \times 10^3$, L/M-cm	$435\text{Å}/392\text{Å}$
PPIXDME	chloroform		407.5	160	
			505.8	14	
			541.1	11	
			575.5	6.5	
			639.9	5.3	
Cd-PPIXDME	chloroform		425.6	200	
			554.0	18	
			590.6	12	
Cd-PPIXDME	dimethyl formamide		433.9	220	
			560.3	22	
Cd-PPIXDME	pyridine		596.0	17	
			431.9	22	
			559.0	22	
			595.9	13	
Cd-PPIX	0.25 M borax buffer	10.0	387.7		
		9.0	385.7		
		8.0	379.4		
		7.0	376.8		
		6.0	358.3		
		5.0	365.9		
		4.0	370.2		
		3.0	370.5		
		2.0	373.5		
			404.5		
Cd-Mb	0.25 M borax buffer	1.0	406.8		
		10.0	435.2	6.0	
		9.0	435.2	6.5	
		8.0	435.2	6.2	
		7.0	435.2	4.5	
		6.0	435.2	3.5	
		5.0	434.9	2.8	
		4.0	343.9	2.4	
3.0	434.9	2.0			
2.0	434.9				

dimethylformamide, respectively, compared with that of protoporphyrin IX dimethyl ester (PPIXDME) (Figure 2a). Absorption maximums and extinction coefficients are summarized in Table I. Incorporation of cadmium results in a 18–27-nm red shift of the Soret band compared to PPIXDME, which is expected from the electron-donating capability of the Cd^{2+} ion to the porphyrin macrocycle relative to that of the protons of the pyrrole nitrogen atoms of the neutral PPIX molecule.¹¹ The

(9) Yonetani, T. *J. Biol. Chem.* **1967**, *242*, 5008.

(10) Marchetti, P. S.; Ellis, P. D.; Bryant, R. G. *J. Am. Chem. Soc.* **1985**, *107*, 8191.

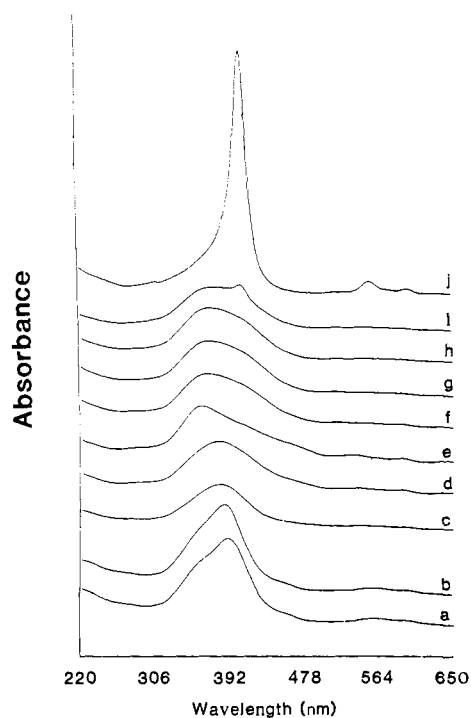


Figure 4. UV-visible spectrum of a 2.8 μM solution of Cd-PPIX in 0.25 M borate buffer at 16 $^{\circ}\text{C}$ at pH = (a) 10.0, (b) 9.0, (c) 8.0, (d) 7.0, (e) 6.0, (f) 5.0, (g) 4.0, (h) 3.0, (i) 2.0, and (j) 1.0 (see Table I).

increased electronic symmetry upon metalation is evident from the reduction of the four-band structure of the PPIXDME to a two-band structure in the metalated porphyrins. In order to establish the "safe" pH region in which to study Cd-PPIX and Cd-Mb by NMR methods, the pH dependence of the UV-visible spectrum of each compound was measured. Figure 4a-h shows that Cd-PPIX remains intact over a pH range between 10.0 and 3.0 though the band shape is sensitive to $[\text{H}^+]$. Samples were prepared by adjusting the pH of the buffer solution with concentrated HCl prior to addition of an aliquot from Cd-PPIX dissolved in pH = 9.4 borate buffer. Table I summarizes the data in Figure 4. However, at pH = 2.0 (Figure 4i), it is evident that Cd-PPIX begins to dissociate into free protoporphyrin IX (PPIX) and Cd^{2+} ion, and by pH = 1.0 the dissociation is complete. The band shape of Cd-Mb, however, is essentially unchanged from pH = 10.0 to pH 6.0, as shown in Figure 5. Solutions were prepared as described above for Cd-PPIX. From pH = 5.0 to pH = 2.0 (Figure 5f-h), increasing dissociation of Cd-Mb into apomyoglobin and Cd-PPIX is evident from the growth of a shoulder in the region where Cd-PPIX is found in that pH range. Finally, at pH = 2.0 (Figure 5i) the predominant species is free PPIX. The binding of Cd-PPIX by the globin apparently protects the cadmium porphyrin from the effects of changing $[\text{H}^+]$ between pH = 6.0 and pH = 10.0 as evidenced by the constancy of the band shape over this pH range.

^{13}C Solution-State NMR. The integrity of Cd-PPIXDME was checked by ^{13}C solution-state NMR spectroscopy. Each carbon resonance in Cd-PPIXDME (Figure 6a) can be assigned by using the previously analyzed ^{13}C spectrum of PPIXDME¹² (Figure 6b). Figure 6 parts c and d show an expansion of the chemical shift scale between 115 and 150 ppm. The broadening of the pyrrole nitrogen carbon resonances due to tautomerization, i.e., proton exchange between the four pyrrole nitrogen atoms in the porphyrin macrocycle, is apparent in Figure 6d. Lincoln and Wray¹³ showed that each pyrrole nitrogen carbon resonance could be resolved by raising the temperature to 87 $^{\circ}\text{C}$. Figure 6c reveals that broadening due to tautomerization is eliminated upon metalation. Also, each of the four chemically distinct vinyl carbon atoms are shown to be intact via the two pairs of resonances at 118 and 130 ppm. A summary of the shift data is shown in Table II.

^1H Solution-State NMR. The vinyl group is the most labile functional group in PPIX.¹⁴ Solutions of PPIX are especially vulnerable to light

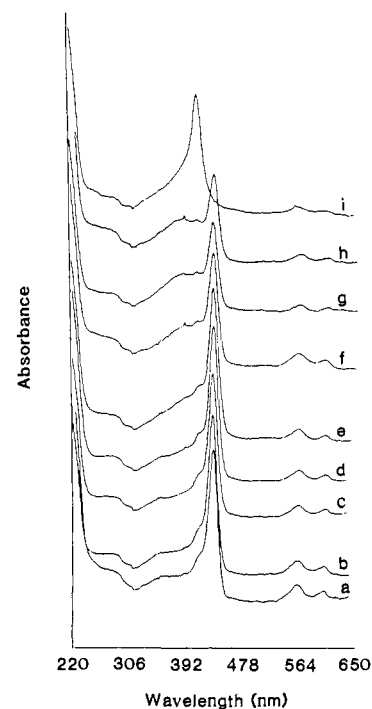


Figure 5. UV-visible spectrum of $\sim 1.0 \mu\text{M}$ solution of Cd-Mb in 0.25 M borate buffer at 16 $^{\circ}\text{C}$ at pH = (a) 10.0, (b) 9.0, (c) 8.0, (d) 7.0, (e) 6.0, (f) 5.0, (g) 4.0, (h) 3.0, and (i) 2.0 (see Table I).

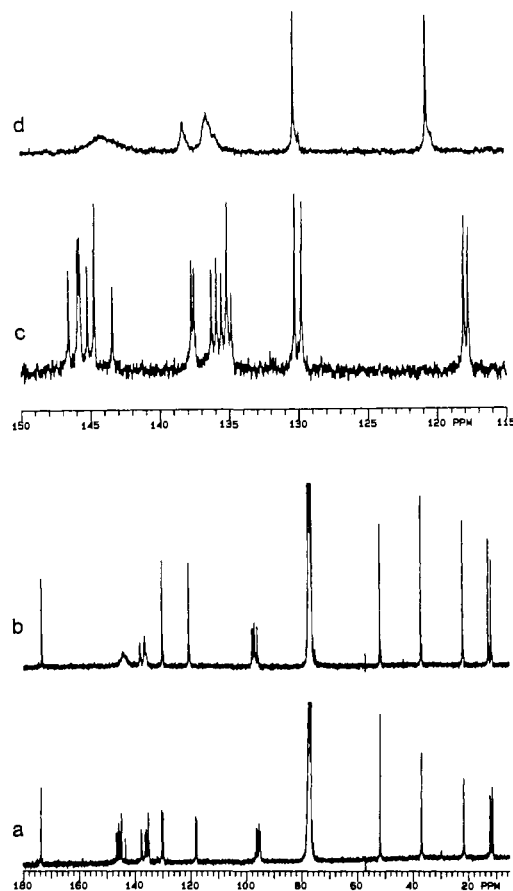


Figure 6. Solution-state 75.4-MHz ^{13}C NMR spectrum of (a) and (c) a 10 mM solution of Cd-PPIXDME (70 000 scans) in $\text{DMF-}d_7$ at 23 $^{\circ}\text{C}$ and (b) and (d) a 10 mM solution of PPIXDME (60 000 scans) in $\text{DMF-}d_7$ at 23 $^{\circ}\text{C}$ at 7.1 T (see Table II) using a 0.410-s acquisition time, 0.5-s, recycle delay, and 30 $^{\circ}$ flip angle (8.0 μs).

as the vinyl groups rapidly photooxidize producing photoporphyrin and isophotoporphyrin.¹⁴ Solution-state ^1H NMR at 300 MHz using a 1 mg/mL solution of Cd-PPIX in deuterated glacial acetic acid

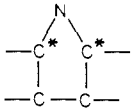
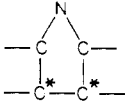
(11) Falk, J. E.; Nyholm, R. S. In *Current Trends in Heterocycle Chemistry*; Albert, A., Badger, G. M., Shopper, C. W., Eds.; Butterworths: London, 1958; p 130.

(12) Battersby, A. R.; Moron, J.; McDonald, E.; Feeney, J. J. *Chem. Soc., Chem. Commun.* **1972**, 920.

(13) Lincoln, D. N.; Wray, V. *Org. Magn. Reson.* **1974**, 6, 542.

(14) Smith, K. M., Ed. *Porphyrins and Metalloporphyrins*; Elsevier: Amsterdam, 1975.

Table II. ^{13}C Chemical Shift Data (DMF- d_7) for Cd-PPIXDME at 75 MHz

carbon group	$\delta(^{13}\text{C}),^a$ ppm
Ar-C*H ₃	11.07, 11.20, 11.77, 12.06
Ar-C*H ₂ CH ₂ COOCH ₃	21.47
Ar-CH ₂ C*H ₂ COOCH ₃	36.66
Ar-CH ₂ CH ₂ COOCH ₃	51.62
meso-C*H	94.83, 95.14, 95.33, 96.14
Ar-CH=C ₂ *	117.69, 118.01
Ar-C*H=CH ₂	129.73, 130.23
	134.80, 135.12, ^b 135.53, 135.88, 136.24, 137.49, 137.68
	143.41, 144.70, ^b 145.21, 145.72, 145.80, 145.88, 146.55
Ar-CH ₂ CH ₂ C*OOCH ₃	173.6

^aPositive chemical shifts are deshielded in ppm relative to tetramethylsilane (TMS). ^bArea of two carbon resonances occurred at this chemical shift.

plus two drops of deuterated sulfuric acid was used to demonstrate that the vinyl protons of Cd-PPIX were intact subsequent to ester hydrolysis. Under these conditions, the Cd²⁺ will dissociate from the porphyrin, however, allowing observation of the porphyrin structure subsequent to the hydrolysis reaction. The four terminal methylene protons were clustered at 6.4 ppm and the two nonterminal methylene protons were clustered at 8.35 ppm. There are two distinct vinyl moieties per porphyrin molecule. The expected 2/1 ratio of areas of terminal vinyl protons to nonterminal protons was observed.

NMR Measurements. Solution-state ^{113}Cd spectra were obtained on a Varian XL-300 spectrometer at 7.1 T and a Varian XL-400 spectrometer at 9.4 T corresponding to ^{113}Cd resonance frequencies of 66.52 and 88.74 MHz, respectively. Varian 10-mm broad-band solution-state probes were used at both fields. All chemical shifts are in ppm relative to 0.1 M Cd (ClO₄)₂ at 20 °C with positive values at lower shielding relative to the standard. Solution-state ^{13}C spectra were obtained on a Varian XL-300 spectrometer at 7.1 T corresponding to a ^{13}C resonance frequency of 75.44 MHz. A Varian 10-mm broad-band solution-state probe was used. Chemical shifts are in ppm relative to TMS with positive values at lower shielding relative to the standard. Solution-state ^1H spectra were obtained on a Varian XL-400 at 9.4 T with a Varian 5-mm probe.

Solid-state CPMAS and static CP ^{113}Cd NMR spectra were obtained by using a standard Hartman-Hahn spin-locked cross-polarization pulse sequence.¹⁵ All solid-state ^{113}Cd NMR experiments were performed on a Varian XL-300 at 7.1 T using a Doty designed MAS probe (Doty Scientific Inc.).

Results and Discussion

Solution-State ^{113}Cd NMR. Cd-PPIXDME. Figure 7 shows the solution-state ^{113}Cd NMR spectrum for Cd-PPIXDME as a function of temperature in CHCl₃. A chemical-exchange process was revealed by lowering the temperature from 20 to -60 °C (see Table III). The identity of the distinct magnetic species is not obvious. If the equilibrium were between a monomer and dimer of Cd-PPIXDME, a 3/1 ratio of peak areas would be expected in the slow exchange. In fact, nearly equal areas are observed for each site. Porphyrins tend to aggregate in solution, mimicking a pseudopolymeric long-range structure. Two distinguishable magnetic sites exist at the Cd²⁺ ion. One site exists via chelation to the four nitrogen atoms of the porphyrin. We propose that the second site is a five-coordinate species where the Cd²⁺ ion is axially coordinated intermolecularly to a carbonyl oxygen from an adjacent propionic ester side chain. In a local region, magnetic site exchange can be thought to occur by the following mechanism. For example, if the polymer chain with the structure proposed above breaks at some point into two polymer chains at time = t_1 , one of the terminal positions of the broken polymer exposes a four-coordinate Cd²⁺ ion which is coordinated to the polymer

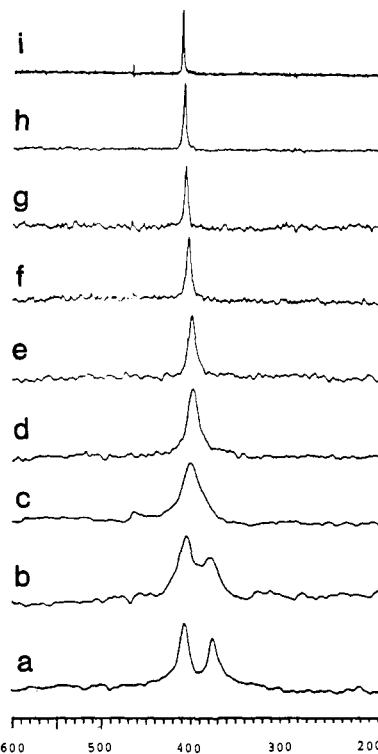


Figure 7. Solution-state 88.7-MHz ^{113}Cd NMR spectrum of a 9.1 mM solution of Cd-PPIXDME in CDCl_3 at (a) -60, (b) -50, (c) -40, (d) -30, (e) -20, (f) -10, (g) 0.0, (h) 10, and (i) 20 °C (see Table III), using 25 000–50 000 scans, 0.150-s acquisition time, 0.300-s recycle delay, and 30° flip pulse (8.0 μs).

Table III. Summary of Solution-State ^{113}Cd NMR Data for Cd-PPIXDME, Cd-PPIX, and Cd-Mb

compd	solvent	T, °C	$\delta(^{113}\text{Cd}),^a$ ppm	mol PYR/mol Cd-PPIXDME
Cd-PPIXDME	chloroform	20	411.5	
		10	408.7	
		0	405.8	
		-10	402.6	
		-20	399.7	
		-30	397.6	
		-40	400.9	
		-50	404.7	
		-60	405.8	
Cd-PPIXDME	dimethyl formamide	25	390.4	0
			393.2	1/2
			414.0	10
			422.0	20
			426.0	30
			433.5	100
Cd-PPIX	70/30, pyridine/20 mol excess aqueous KOH	30	431.7	
		25	432.2	
		20	432.3	
		15	432.4	
		10	432.7	
Cd-PPIX	0.1 M bicarbonate buffer (pH = 10.5)	5	433.1	
		3.5	345.0	
Cd-Mb	0.1 M borax buffer (pH = 9.4)	30	449.7	
		25	450.5	
		20	451.2	
		15	451.8	
		10	452.5	
		5	453.1	

^aPositive chemical shift in ppm deshielded relative to 0.1 M aqueous CdClO₄ at 20 °C.

through a carboxylate carbonyl group on the porphyrin. The complementary terminus of the second residual polymer chain exposes a five-coordinate Cd²⁺ ion which is coordinated to the polymer chain through an axial interaction with a carboxyl

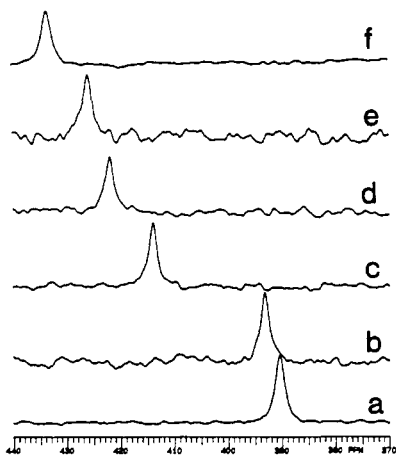


Figure 8. Solution-state 66.5-MHz ¹¹³Cd NMR spectrum of a 24 mM solution of Cd-PPIXDME in DMF-*d*₇ at 23 °C in the presence of (a) 0.0, (b) 1/2, (c) 10, (d) 20, (e) 30, and (f) 100 mol ratio of pyridine to Cd-PPIXDME (see Table III) using 25 000–50 000 scans, 0.513-s acquisition time, 0.0-s recycle delay, and 30° flip pulse (8.0 μs).

carbonyl group from another porphyrin molecule. At some later time $t_1 + \Delta t$, the exposed terminal sites are filled by other available polymer terminal sites. This local scheme can be envisioned to occur randomly over the macroscopic volume of the sample. Given this scenario, roughly equal peak areas for each environment would be expected in slow exchange. The problem reduces accordingly to a simple two-site exchange. The shielding of the resonance from 411.5 ppm (Figure 7i) to 397.7 ppm (Figure 7d) as the temperature is lowered from 20 to -30 °C is consistent with the expected shift in equilibrium toward the five-coordinate oxo species as the temperature is decreased. The increased line width from 133 Hz at 20 °C (Figure 7i) to 2024 Hz at -40 °C (Figure 7c) indicates the system is now in an intermediate exchange regime. Near the fast-exchange regime, for a simple two-site exchange, $A \rightleftharpoons X$, with equal populations, a single Lorentzian line is observed with a line width given by¹⁶

$$\Delta\nu_{1/2} = \frac{1}{2}\pi(\nu_A - \nu_X)^2 k_r^{-1} \quad (1)$$

Using the line width and eq 1, the approximate rate constants were determined in the fast-exchange regime. At 20 °C, $k_r = 9.4 \times 10^4$ Hz which corresponds to a lifetime $\tau_A = 10$ μs. At coalescence, i.e., -40 °C (Figure 7c), $k_r = 6.2 \times 10^3$ Hz and $\tau_a = 160$ μs. The rate constants at each temperature were used to calculate the activation energy, $E_A = 6.0 \pm 0.05$ kcal/mol, for the association of two terminal sites in the polymer. Below the coalescence temperature at -40 °C, two resolvable resonances are observed at 405.8 and 374.0 ppm (Figure 7a). The resonance at 405.8 ppm is assigned to the four nitrogen coordinate site and the resonance at 374.0 to the five-coordinate oxo species. The averaged resonance in fast exchange at 20 °C is at 411.5 ppm, whereas the average of the resolved resonances at -60 °C is at 389.9 ppm. The chemical shift is likely due to the complexity of the equilibrium.

The titration of Cd-PPIXDME with pyridine, shown in Figure 8, clearly indicates an exchange process for the reaction $\text{Cd-PPIXDME} + \text{PYR} \rightleftharpoons \text{Cd-PPIXDME-PYR}$. K_{eq} for this equilibrium is defined by eq 2. Here, the presence of a single $K_{\text{eq}} = [\text{Cd-PPIXDME-PYR}] / [\text{Cd-PPIXDME}][\text{PYR}]$ (2)

resonance is indicative of a system that is undergoing fast exchange. Therefore, the observed chemical shift is governed by eq 3,¹⁶ i.e., the averaged chemical shift is determined by the ratio

$$\delta_{\text{obsd}} = \chi_f \delta_f + (1 - \chi_f) \delta_b \quad (3)$$

of the mole fraction of free porphyrin, $\chi_{\text{Cd-PPIXDME}}$, to that of the ligand-bound porphyrin, $\chi_{\text{Cd-PPIXDME-PYR}}$. The sequential addition of up to a 100 mol excess of pyridine alters the mole fractions $\chi_{\text{Cd-PPIXDME}}$ and $\chi_{\text{Cd-PPIXDME-PYR}}$, resulting in a change in the

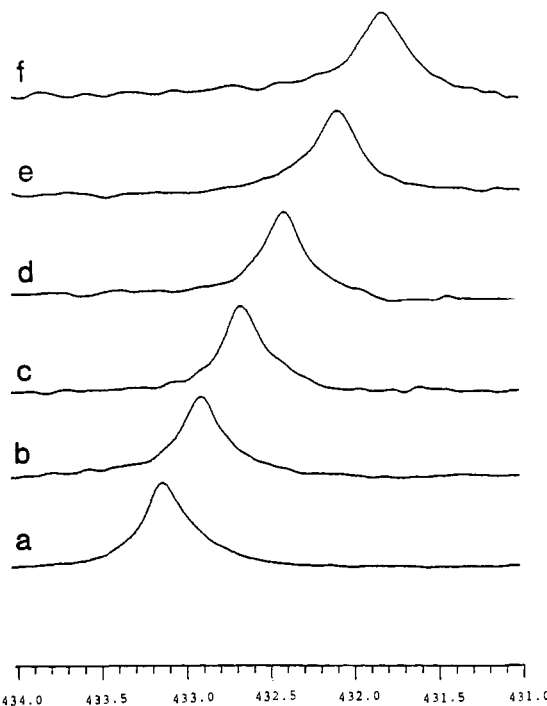


Figure 9. Solution-state 66.5-MHz ¹¹³Cd NMR spectrum of a 6.4 mM solution of Cd-PPIX in 70/30 pyridine/KOH (20% mole excess of OH⁻) at (a) 5, (b) 10, (c) 15, (d) 20, (e) 25, (f) 30 °C (see Table III) using 5000–15 000 scans, 0.205-s acquisition time, 0.0-s recycle delay, and 30° flip pulse (8.0 μs).

observed chemical shift. A 43 ppm span of averaged chemical shift (see Table III) occurred over the course of the titration. A Scatchard plot analysis of this data yields an equilibrium dissociation constant $K_d = 0.22 \pm 0.02$ M. Therefore, in the presence of pyridine the five-coordinate pyridyl adduct of Cd-PPIXDME is favored. Also, the extrapolation to infinite pyridine concentration yields a maximum shift of 45.0 ppm on binding of pyridine to Cd-PPIXDME. Thus, the isotropic chemical shift for the completely ligated complex would be expected at 435.5 ppm.

Cd-PPIX. The solution-state ¹¹³Cd NMR spectrum of Cd-PPIX in 70/30 pyridine/aqueous KOH (20% mole excess OH⁻) is shown in Figure 9 for a temperature range between 5 and 30 °C. A single resonance, 431.7–432.9 ppm (Table III), is observed whose line width of 32 ± 5 Hz is temperature independent over the range studied. The temperature dependence of the chemical shift is due to chemical exchange between a four-coordinate Cd²⁺ ion liganded to the porphyrin and a five-coordinate Cd²⁺ ion in which pyridine is coordinated in the axial position. Evidence that pyridine coordinates as a fifth ligand to the Cd²⁺ is (1) that in the absence of pyridine in NaHCO₃ buffer the Cd-PPIX resonance occurs at 345 ppm and (2) the deshielding by 89 ppm of Cd-PPIXDME by titration with pyridine (see Table III). The titration of Cd-PPIXDME with pyridine altered the mole fraction ratio by addition of pyridine at constant temperature. In this experiment, the amount of available pyridine is fixed while the temperature is changed. The ratio of free to ligand-bound porphyrin is governed at equilibrium by the expression for the thermal equilibrium constant, K_{eq} . The equilibrium constant is, from Gibb's free energy equation, temperature dependent. Specifically, if the association constant for $\text{Cd-PPIX} + \text{PYR} \rightleftharpoons \text{Cd-PPIX-PYR}$ is used then K_{eq} , as defined in eq 4, is proportional to the antilog-

$$K_{\text{eq}} = [\text{Cd-PPIX-PYR}] / [\text{Cd-PPIX}][\text{PYR}] \quad (4)$$

arithm of the inverse of temperature. When the temperature is lowered, the equilibrium position shifts in favor of Cd-PPIXDME-PYR. The deshielding at lower temperature is consistent with the deshielding influence expected by pyridine ligation as shown by the pyridine titration of Cd-PPIXDME.

Although the temperature dependence of the isotropic chemical shift is adequately explained by a chemical equilibrium argument,

(16) Harris, R. K. *Nuclear Magnetic Resonance Spectroscopy*; Pitman: London, 1983.

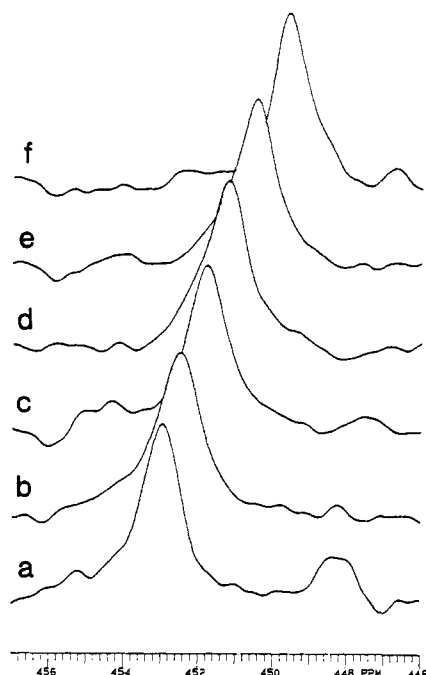


Figure 10. Solution-state 66.5-MHz ^{113}Cd NMR spectrum of a 5 mM solution of Cd-Mb in 0.1 M borate buffer at pH = 9.4 at (a) 5.0, (b) 10, (c) 15, (d) 20, (e) 25, and (f) 30 °C (see Table III) using 100 000–150 000 scans, 0.155-s acquisition time, 0.0-s recycle delay, and 30 flip angle (8.0 μs).

the observed resonance contains an intrinsic temperature dependence in the local paramagnetic contribution to the chemical shift. The paramagnetic temperature dependence originates from population changes of the electronic states of the atom due to the temperature-dependent mixing of electronic states in the presence of a strong external magnetic field.¹⁶ Paramagnetic contributions become significant in transition metals such as cobalt in which, from ligand field theory, electronic energy spacing for a $3d^6$ electronic configuration between occupied and unoccupied orbitals is small. The Cd^{2+} ion has a valence configuration of $4d$,¹⁰ and the large electronic excitation energy results in a negligible probability that mixing will occur over the temperature range studied.

Cd-Mb. The solution-state ^{113}Cd NMR spectrum of Cd-Mb is shown in Figure 10 as a function of temperature. A single resonance is observed whose line width of 47 ± 5 Hz is independent of temperature. The observed 3.4 ppm chemical shift ranges from 449.7 to 453.1 ppm between 5 and 30 °C (Table III), respectively, with greater shielding at higher temperature, which is directly analogous to the previously discussed cadmium-porphyrin data. Therefore, it can be concluded that the Cd^{2+} ion in Cd-Mb is undergoing fast chemical exchange in which the temperature-dependent chemical shift reflects a change in the equilibrium position. Cd-PPIX remains noncovalently bound to the protein while the Cd^{2+} ion participates in an equilibrium between four-coordinate Cd-PPIX, i.e., no axial interaction, and five-coordinate Cd-PPIX axially coordinated to a proximal histidyl nitrogen atom. The isotropic chemical shift of Cd-Mb is deshielded by approximately 20 ppm relative to Cd-PPIX in an aqueous pyridine solution. This chemical shift could be in part due to (a) stronger Lewis basicity of histidine compared to pyridine¹⁷ or (b) different Cd-N bond lengths resulting from steric constraints associated with the ligand structures. Based on correlation times on the order of 10^{-10} s for Cd-TPP and PY-Cd-TPP,⁶ typical correlation times on the order of tens of nanoseconds for macromolecules, and the roughly equivalent magnitude in shielding anisotropies, a factor of 150 increase in line width is expected for binding of Cd-PPIX

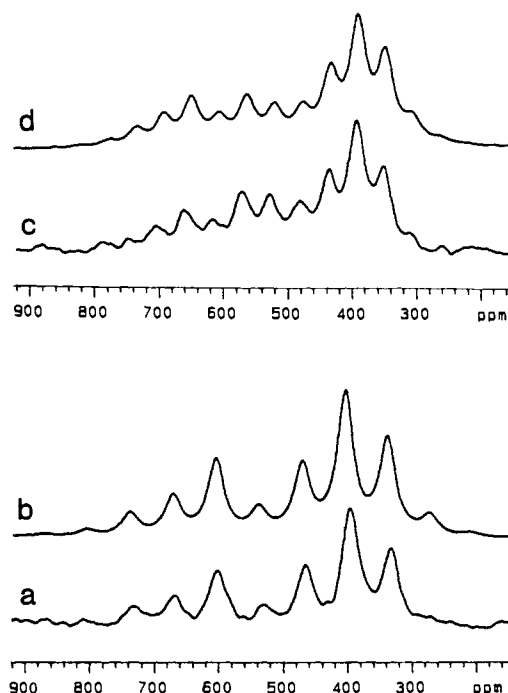


Figure 11. Solid-state CPMAS 66.5-MHz ^{113}Cd NMR spectrum of Cd-PPIXDME (a) at 4320 Hz spinning rate (16914 scans), 0.020-s acquisition time, 7.0-ms contact time, 2.0-s recycle delay, (b) simulated MAS spectrum using optimized parameters, $\eta = 0.01$, $\Delta\sigma = +432$ ppm, 4320 Hz spinning rate and 1500 Hz artificial line broadening, (c) at 2952 Hz spinning rate (16914 scans), 0.020-s acquisition time, 7.0-ms contact time, 2.0-s recycle delay, and (d) simulated MAS spectrum using optimized parameters, $\eta = 0.01$, $\Delta\sigma = +432$ ppm, 2952 Hz spinning rate, and 1500 Hz artificial line broadening (see Table IV).

to apomyoglobin. However, only a 30% increase is observed. The smaller than expected change is likely due to a longer correlation time for Cd-PPIX-PYR compared to Py-Cd-TPP, which is consistent with the greater tendency of protoporphyrin IX to aggregate in aqueous solution compared to tetraphenylporphyrin in organic solvents.¹⁷

Solid-State ^{113}Cd NMR. Cd-PPIXDME. The solid-state ^{113}Cd NMR CPMAS spectra of Cd-PPIXDME, shown in Figure 11a, reveal a single chemical shift tensor with isotropic chemical shift of 480 ppm, which is ~ 90 ppm deshielded relative to Cd-PPIXDME in DMF solution. In solution, solvent coordination through the amide carbonyl oxygen in fast exchange may account for shielding relative to solid Cd-PPIXDME. The average line width of ~ 1500 Hz includes a contribution of J splitting of the cadmium coupled to four nitrogen atoms which is not averaged by magic-angle spinning and direct dipolar coupling of cadmium to each of the quadrupolar ^{14}N atoms in the chelating porphyrin ligand. The best estimate of the chemical shielding tensor parameters was obtained by the method of Marchetti et al.¹⁰ which fits the spinning side-band intensities after the theory of Maricq and Waugh.¹⁹ The resultant fit is shown in Figure 11b. Axial symmetry is indicated by the $\eta = 0.01$ asymmetry parameter and is reflected by the static powder pattern shown in Figure 15a. The Cd^{2+} ion must, therefore see a local pseudofourfold rotation axis perpendicular to the porphyrin plane. Based on the molecular symmetry we can make the assignment that the unique tensor element, σ_{\parallel} , should be along the pseudofourfold axis and the nonunique tensor elements, σ_{\perp} , should be in the plane perpendicular to the symmetry axis. Rigorously, only a center of inversion can exist. The anisotropy, $\Delta\sigma$, which was determined to be 432 ppm, indicates that in-plane vs axial electronic perturbation to the Cd^{2+} atom due to bonding is dramatically different. The orientation and magnitude of a shielding tensor element is determined by the current density in the plane perpendicular to that

(17) Munakata, M.; Kitagawa, S.; Yagi, F. *Inorg. Chem.* **1986**, *25*, 964.

(18) Lacelle, S.; Stevens, W.; Kurtz, D., Jr.; Richardson, J. W., Jr.; Jacobsen, R. A. *Inorg. Chem.* **1984**, *23*, 930.

(19) Maricq, M.; Waugh, J. J. *J. Chem. Phys.* **1979**, *70*, 3300.

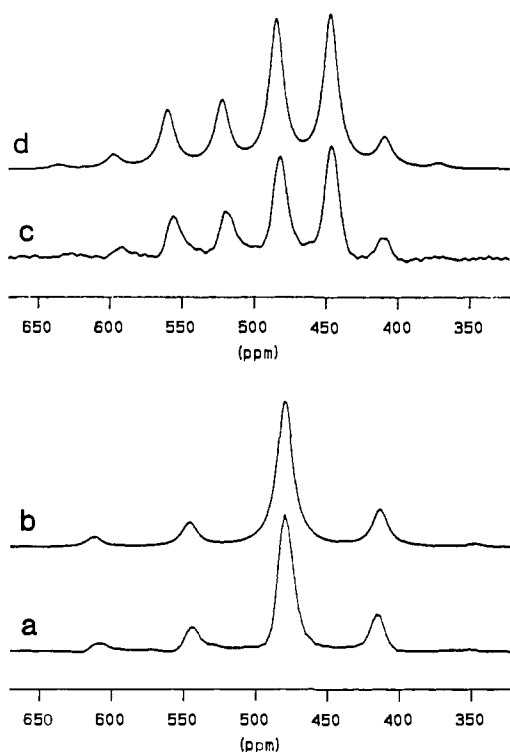


Figure 12. Solid-state CPMAS 66.5-MHz ^{113}Cd NMR spectrum of Cd-PPIXDME-PYR (a) at 4373 Hz spinning rate (4575 scans), 0.003-s acquisition time, 5.0-ms contact time, 4.0-s recycle delay, (b) simulated MAS spectrum using optimized parameters, $\eta = 0.32$, $\Delta\sigma = +163$ ppm, 4373 Hz spinning rate, and 1200 Hz artificial line broadening, (c) at 2525 Hz spinning rate (5683 scans), 0.003-s acquisition time, 5.0-ms contact time, 4.0-s recycle delay, and (d) simulated MAS spectrum using optimized parameters, $\eta = 0.32$, $\Delta\sigma = +163$ ppm, 2525 Hz spinning rate, and 1200 Hz artificial line broadening (see Table IV).

element. Therefore, the in-plane porphyrin-Cd bonding manifests itself in the unique shielding tensor element, $\sigma_{\parallel} = 770$ ppm. Jakobsen et al.⁶ reported $\sigma_{\parallel} = 626$ ppm for Cd-TPP, which is shielded by 144 ppm relative to σ_{\parallel} for Cd-PPIXDME and reflects exceptionally strong in-plane covalent interactions in Cd-PPIXDME. A redistribution of π charge density into the polar side chains in Cd-PPIXDME allowing more significant overlap with the Cd^{2+} ion than in Cd-TPP may explain these results. The ionic radius of Cd^{2+} is 0.92 Å, whereas the largest radius accommodated by the chelating porphyrin ligand is ≈ 0.75 Å². The Cd^{2+} ion must, therefore, lie above the porphyrin plane yet allow significant overlap of its $5p_x$ and $5p_y$ bonding orbitals with the molecular orbitals of the porphyrin ligand. The nonunique elements, σ_{\perp} , are shielded by 432 ppm relative to σ_{\parallel} and reflect the absence of perturbation by an axial donor ligand.

Cd-PPIXDME-PYR. The solid-state CPMAS ^{113}Cd NMR spectra of the pyridyl adduct of Cd-PPIXDME along with simulated spectra are shown in Figure 12. A single chemical shift tensor is observed with an isotropic chemical shift of 480 ppm, which is deshielded by 45 ppm relative to the extrapolated solution-state value. The exact origin of this chemical shift difference is not clear. The Cd^{2+} -pyridine bond distance may be shorter in the solid state. The static powder spectrum of Cd-PPIXDME-PYR shown in Figure 15b has a small asymmetry, $\eta = 0.32$. The discontinuities between σ_{11} and σ_{22} (see Table IV) are not resolved due to dipolar broadening of the powder pattern. The nonzero asymmetry parameter indicates that the pseudo-fourfold symmetry axis is reduced upon pyridine ligation. If pyridine were oriented normal to the porphyrin plane, the local symmetry would remain a pseudofourfold rotation axis which would result in an asymmetry parameter equal to zero. This is not observed. The symmetry has therefore been reduced to less than a fourfold symmetry axis. If the pyridine molecule coordinated at the Cd^{2+} site is tipped away from normal to the plane,

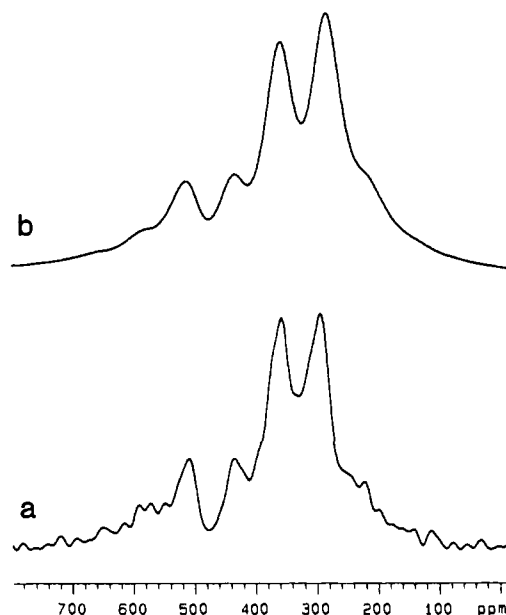


Figure 13. Solid-state CPMAS 66.5-MHz ^{113}Cd NMR spectrum of Cd-PPIX (a) at 4723 Hz spinning rate (13012 scans), 0.002-s acquisition time, 5.0-ms contact time, and 4.0-s recycle delay and (b) simulated MAS spectrum using optimized parameters, $\eta = 0.06$, $\Delta\sigma = +302$ ppm, 4723 Hz spinning rate, and 3500 Hz artificial line broadening (see Table IV).

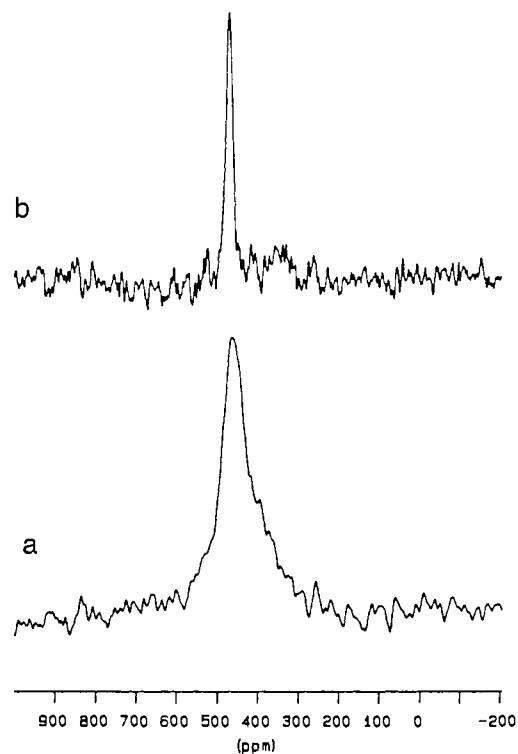


Figure 14. Solid-state CPMAS 66.5-MHz ^{113}Cd NMR spectrum of Cd-Mb (a) lyophilized and spinning at 4130 MHz (43 776 scans), 0.068-s acquisition time, 4.0-ms contact time, 2.0-s recycle delay and (b) D_2O -equilibrated (0.2 g of D_2O /g of protein) Cd-Mb spinning at 3.5 KHz (14 337 scans), 0.068-s acquisition time, 4.0-ms contact time, 2.0-s recycle delay (see Table IV).

possibly due to steric stress caused by stacking of the porphyrin molecules, reduced symmetry would result.

The isotropic chemical shift of Cd-PPIXDME-PYR is identical with that of Cd-PPIXDME in the solid state. If only this information were available, pyridine ligation would appear to have only a small effect on the chemical shift of Cd-PPIXDME. Comparison of the static powder spectra of Cd-PPIXDME-PYR

Table IV. Chemical Shielding Tensor Parameters of Model Compounds for Cd-hemoglobin

compd	tensor elem, ^a ppm	anisotr $\Delta\sigma$, ^a ppm	asym η	
Cd-PPIXDME	σ_{11}	336	432	0.01
	σ_{22}	338		
	σ_{33}	770		
	$\bar{\sigma}$	480		
Cd-PPIXDME-PYR	σ_{11}	407	163	0.32
	σ_{22}	442		
	σ_{33}	588		
	$\bar{\sigma}$	480		
Cd-PPIX-K ₂	σ_{11}	263	301	0.06
	σ_{22}	265		
	σ_{33}	566		
	$\bar{\sigma}$	365		
Cd-myoglobin	σ_{11}	330	≈ -200	0.0-0.4
	σ_{22} ^b	≈ 355		
	σ_{33}	520		
	$\bar{\sigma}$	467		

^a Positive chemical shift is deshielded relative to solid CdClO₄. ^b The value of σ_{22} was estimated by using $\eta = 0.2$.

(Figure 15b) with Cd-PPIXDME (Figure 15a) reveals that large compensating changes of the in-plane and unique shielding tensor elements result in zero chemical shift between the two compounds. The "orthogonal" nature of the shielding interaction has been previously discussed clearly by Jakobsen et al.⁶ for the analogous pair of compounds Cd-TPP and PY-Cd-TPP. A summary of this discussion is appropriate for the comparison of Cd-PPIXDME-PYR with Cd-PPIXDME. The orientation of a chemical shielding tensor element is determined by the current density in the plane perpendicular to that element. Therefore, if the pyridine were to coordinate to the cadmium simply thru the 5p_z orbital (or appropriate combination of orbitals) without any further geometrical distortion, only a minor change in the unique shielding tensor element would be expected while a large change in the nonunique shielding tensor elements would be expected. However, if the pyridyl adduct pulls the cadmium out of the plane, then large changes in all the shielding tensor elements are expected. Comparison of Cd-PPIXDME-PYR in Figure 15b with Cd-PPIXDME in Figure 15a shows that large changes in both the in-plane and unique tensor elements accompany pyridine coordination. Therefore, the Cd²⁺ ion is pulled further out of the porphyrin plane with pyridyl coordination in Cd-PPIXDME. The resulting anisotropy of 163 ppm is 2.5 times smaller than that of Cd-PPIXDME. The decreased anisotropy correlates with more similar in-plane and axial bonding interactions in Cd-PPIXDME-PYR than in Cd-PPIXDME. The most shielded tensor elements in Cd-PPIXDME-PYR occur at 407 and 442 ppm compared to 337 ppm in Cd-PPIXDME. These correspond to the in-plane tensor elements which are determined by the bonding interaction perpendicular to the plane. The axial ligation of pyridine is deshielding relative to when there is no axial ligand. Congruently, the most deshielded element in Cd-PPIXDME-PYR is $\sigma_{33} = 588$ ppm compared to $\sigma_{33} = 770$ ppm in Cd-PPIXDME. The unique tensor element is determined by the in-plane bonding interaction. The more shielded unique element in Cd-PPIXDME-PYR indicates that the in-plane covalent bonding interaction is weakened relative to that in Cd-PPIXDME, which is consistent with the pulling of the cadmium atom out of the plane by the axial ligation of pyridine.

Cd-PPIX. The solid-state CPMAS ¹¹³Cd NMR spectra of Cd-PPIX, shown in Figure 13a, exhibits a single shielding tensor with isotropic chemical shift, $\sigma = 365$ (see Table III). The solid sample of Cd-PPIX was collected in the form of an amorphous precipitate, likely comprised of a distribution of aggregated dimers and polymers. The broad lines of ~ 2000 Hz are likely due to chemical shift dispersion reflecting the amorphous nature of the sample. Besides stacking effects, there may be intermolecular coordination of carboxylate anions to axial coordination sites which could account for the shielding of the isotropic shift by ~ 115 ppm relative to Cd-PPIXDME and Cd-PPIXDME-PYR. The $\eta =$

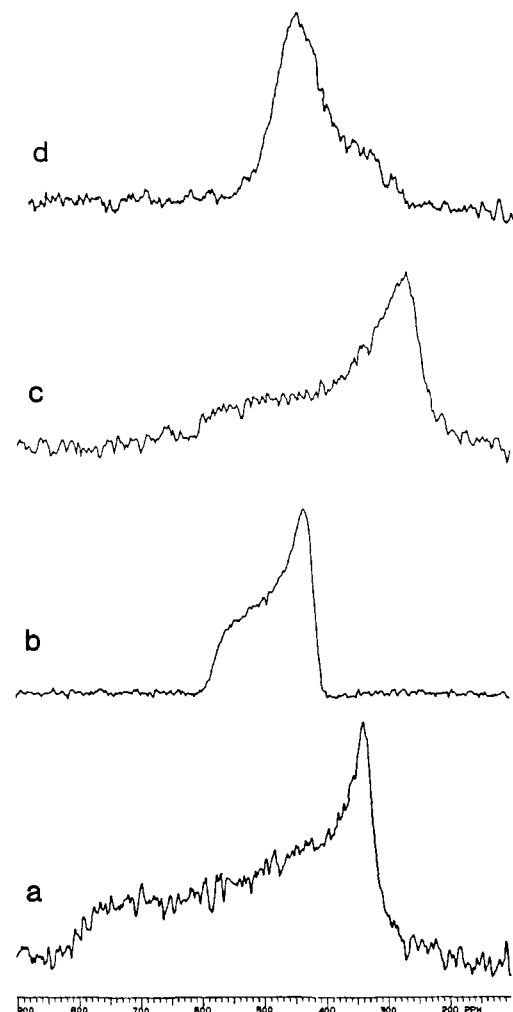


Figure 15. Solid-state static powder 66.5-MHz ¹¹³Cd NMR spectrum of (a) Cd-PPIXDME (16 914 scans), 0.013-s acquisition time, 7.0-ms contact time, 3.0-s recycle delay, (b) Cd-PPIXDME-PYR (9308 scans), 0.003-s acquisition time, 5.0-m contact time, 4.0-s recycle delay, (c) Cd-PPIX (11 479 scans), 80- μ s acquisition time, 5.0-ms contact time, 8.0-s recycle delay, and (d) lyophilized Cd-Mb (45 313 scans), 0.026-s acquisition time, 4.0-ms contact time, 6.0-s recycle delay (see Table IV).

0.01 chemical shift tensor results in a static powder line shape shown in Figure 15c which is broadened due to aggregation. The small asymmetry indicates that the Cd²⁺ ion again sees a pseudofourfold symmetry axis. The anisotropy of 261 ppm is intermediate between Cd-PPIXDME and Cd-PPIXDME-PYR. The most shielded tensor elements, $\sigma = 277$ ppm, are ~ 110 ppm shielded relative to those in Cd-PPIXDME and ~ 225 ppm shielded relative to those in Cd-PPIXDME-PYR. Thus, the axial electronic perturbation in Cd-PPIX, which is still significant relative to normal oxygen ligation,²⁰ is much smaller than either of the other porphyrins. Also, the most deshielded element, $\sigma = 539$ ppm, is shielded by ~ 50 ppm compared to Cd-PPIXDME-PYR and 230 ppm compared to Cd-PPIXDME. These data indicate that the molecular orbital structure in PPIX is such that covalent coordination to Cd²⁺ is weaker than in either of the porphyrin ester complexes.

Cd-Mb. The solid-state CPMAS ¹¹³Cd NMR spectrum of lyophilized Cd-Mb (Figure 14a) and D₂O-equilibrated Cd-Mb (Figure 14b) reveals a single chemical shift tensor with an isotropic chemical shift, $\sigma = 467$ ppm, which is deshielded by ~ 15 ppm relative to Cd-Mb in solution. Chemical exchange may account for this chemical shift. The CPMAS spectrum of Cd-Mb in

(20) (a) Honkonen, R. S.; Doty, F. D.; Ellis, P. D. *J. Am. Chem. Soc.* **1983**, *105*, 4163. (b) Honkonen, R. S.; Ellis, P. D. *J. Am. Chem. Soc.* **1984**, *106*, 5488.

Figure 14b was not reproducible due to decomposition of Cd-Mb with high-speed MAS spinning. Apparently, the centrifugal pressure compressed the D₂O-reequilibrated protein beyond that which its structure could withstand. The original moist powder of D₂O-equilibrated Cd-Mb was transformed into an insoluble, hard, polymeric material upon spinning. We are currently trying to obtain MAS spectra of the quality needed for fitting by simulation. The static powder ¹¹³Cd NMR spectrum of Cd-Mb is shown in Figure 15d. We have estimated the shielding tensor parameters from the powder spectrum and they are summarized in Table IV. Although disorder of the porphyrin in the heme pocket may result in less well resolved discontinuities of the powder pattern, it is immediately evident that the anisotropy of the chemical shift tensor has changed sign relative to Cd-PPIXDME, Cd-PPIXDME-PYR, and Cd-PPIX. The in-plane tensor elements, $\sigma_{\perp} \approx 520$ ppm, are now deshielded relative to the unique element, $\sigma_{\parallel} = 330$ ppm, which is opposite to all previous examples of pyridyl adducts of cadmium porphyrins.⁶ The isotropic chemical shift of Cd-PPIXDME-PYR, which most closely models Cd-Mb, is deshielded by only 13 ppm relative to solid Cd-Mb. In solution state, the isotropic shift of Cd-PPIXDME-PYR is shielded by 18 ppm relative to Cd-Mb. Again, if only the solution-state data were available, we would conclude, incorrectly, that Cd-PPIXDME-PYR and Cd-Mb were very similar structurally and electronically. The power of solid-state NMR is again demonstrated by exploiting the information contained in the shielding tensor parameters. In this case, solid-state ¹¹³Cd NMR sensitively distinguishes pyridine from a protein histidine residue as an axial fifth ligand to Cd-PPIX, not by the isotropic chemical shift but by the sign of the anisotropy. In the case of Cd-PPIXDME, axial pyridine coordination results in shielding of the unique tensor element by 182 ppm and deshielding of the in-plane elements by ~ 83 ppm, i.e., the tensor elements have moved toward each other on the chemical shift scale. If the strength of the axial interaction is increased beyond that of an axial pyridine ligand, one can envision the tensor elements crossing over at some point. In

Cd-Mb, the histidyl residue coordinates axially through nitrogen to the cadmium atom in such a way as to cause such a crossover to occur. The strong axial Cd-N interaction is not completely surprising, since in native myoglobin the Fe-N bond is the single covalent interaction through which the prosthetic porphyrin molecule is bound to the globin.

Conclusions

Solution- and solid-state ¹¹³Cd NMR parameters have been measured in order to characterize dynamical and structural consequences of axial ligation in Cd²⁺-coordinated protoporphyrin IX complexes, i.e., immediate precursors of Cd²⁺-substituted hemoglobins. Solution-state results indicate that the Cd²⁺ ion undergoes fast exchange in Cd-Mb with and without axial proximal histidyl nitrogen coordination to the cadmium porphyrin. In the solid state, axial coordination of histidine to Cd-PPIX results in an anisotropy of ~ 200 ppm, whereas axial coordination of pyridine to Cd-PPIXDME is distinguished by an anisotropy of $+163$ ppm. The change in the sign of the anisotropy reflects the difference in (1) the Lewis basicity of the axial ligand and (2) the Cd-axial ligand bond length. Therefore, solid-state ¹¹³Cd NMR has been shown to be sensitive to the presence, identity, and bond length of the axial coordination ligands to cadmium porphyrins. In future work, cadmium porphyrins should provide a novel probe with which to examine axial dynamical and structural changes in Cd²⁺-substituted hybrid hemoglobins. Furthermore, the expansion of solution- and solid-state ¹¹³Cd NMR into investigation of other hemoproteins is promising.

Acknowledgment. We gratefully acknowledge the support from the National Institutes of Health via Grant GM26295. Further, we would like to acknowledge the helpful suggestions of Drs. Paul Marchetti and Raja Khalifah.

Registry No. Cd-PPIXDME, 14729-09-0; Cd-PPIX, 80216-25-7; PPIXDME, 5522-66-7; Cd-PPIXDME-PYR, 119818-85-8; PYR, 110-86-1; ¹¹³Cd, 14336-66-4.

Model Systems for Rhodopsins: The Photolysis of Protonated Retinal Schiff Bases, Cyanine Dye, and Artificial Cyanine-Bacteriorhodopsin

Noga Friedman,[†] Mordechai Sheves,^{*†} and Michael Ottolenghi^{*†}

Contribution from the Department of Organic Chemistry, The Weizmann Institute of Science, Rehovot 76100, Israel, and the Department of Physical Chemistry, The Hebrew University of Jerusalem, Jerusalem 91904, Israel. Received September 6, 1988

Abstract: Protonated Schiff bases of retinal (RSBH⁺), of its (planar) linear polyene analogue 1,1-didemethylretinal (LRSBH⁺), and of an analogous cyanine dye (Cy^{III}) are submitted to pulsed laser photolysis over a range of solvents and temperatures. Transient phenomena observed with the Cy^{III} dye are attributed to trans \rightarrow cis isomerization, followed by secondary excitation which induces rotation about an additional bond. In the cases of RSBH⁺ and LRSBH⁺ (photostationary mixtures of cis-trans isomers), laser excitation of deaerated solutions leads to the observation of triplet states. The latter are formed via intersystem crossing (ISC) from a short-lived excited state, generated by multiple excitations of the ground state during the (same) intense laser pulse. O₂ saturation of the solutions suppresses the ISC route, giving rise to a short-lived phototransient observed at low temperatures, which is identified as a C-C conformer. The observations are discussed in light of the possibility that C-C conformers may play a role in the photocycles of visual rhodopsins and of bacteriorhodopsin. Experiments were also performed with an artificial bacteriorhodopsin pigment (bR_{Cy}) carrying a cyanine chromophore analogous to Cy^{III}. A single photointermediate (bR_{Cy}/I), reminiscent of the K phototransient of bR, is observed and is attributed to a cis isomer. The low activation and preexponential parameters which characterize the thermal relaxation of bR_{Cy}/I are discussed in terms of cis \rightarrow trans isomerization in a rhodopsin binding site. The results bear on the thermal 13-cis \rightarrow all-trans relaxation in the final stages of the bR photocycle and on the inefficiency of a back (all-trans \rightarrow 11-cis) reaction at the early (bathorhodopsin) stage of the visual photocycle.

Visual pigments and bacteriorhodopsin (bR), the purple-membrane pigment in the photosynthetic microorganism *Halo-bacterium halobium*, are both composed of a retinylpolyene

chromophore bound to the parent protein (opsin) via a protonated Schiff base bond with a lysine residue. It is now well established that in both systems the photocycle is initiated by primary isom-